Journal of Pharmaceutical and Biomedical Analysis 88 (2014) 269–277

Contents lists available at ScienceDirect

Journal of Pharmaceutical and Biomedical Analysis

journal homepage: www.elsevier.com/locate/jpba

Simultaneously enantiospecific determination of (+)-*trans*-khellactone, (+/−)-praeruptorin A, (+/−)-praeruptorin B, (+)-praeruptorin E, and their metabolites, (+/−)-*cis*-khellactone, in rat plasma using online solid phase extraction–chiral LC–MS/MS

Yuelin Song[a], Wanghui Jing[a], Fengqing Yang[b], Zhan Shi[c], Meicun Yao[c], Ru Yan[a], Yitao Wang[a,*]

[a] State Key Laboratory of Quality Research in Chinese Medicine, Institute of Chinese Medical Sciences, University of Macau, 999078, Macao
[b] School of Chemistry and Chemical Engineering, Chongqing University, 401331 Chongqing, China
[c] School of Pharmaceutical Sciences, Sun Yat-sen University, 510006 Guangzhou, China

ARTICLE INFO

Article history:
Received 31 May 2013
Received in revised form 21 August 2013
Accepted 28 August 2013
Available online 7 September 2013

Keywords:
Online SPE
Chiral LC–MS/MS
Enantiospecific
Peucedani Radix
Pharmacokinetics

ABSTRACT

Many chiral drugs are used as the racemic mixtures in clinical practice. The occurrence of enantioselectively pharmacological activities calls for the development of enantiospecific analytical approaches during pharmacokinetic studies of enantiomers. Sample preparation plays a key role during quantitative analysis of biological samples. In current study, a rapid and reliable online solid phase extraction–chiral high performance liquid chromatography–tandem mass spectrometry (online SPE–chiral LC–MS/MS) method was developed for the simultaneously enantiospecific quantitation of (+)-*trans*-khellactone (*d*TK), (+/−)-*cis*-khellactone (*d*/*l*CK), (+/−)-praeruptorin A (*d*/*l*PA), (+/−)-praeruptorin B (*d*/*l*PB) and (+)-praeruptorin E (*d*PE), the main active angular-type pyranocoumarins (APs) in Peucedani Radix (Chinese name: Qian-hu) or the major metabolites of those APs, in rat plasma. The validation assay results described here show good selectivity and enantiospecificity, extraction efficiency, accuracy and precision with quantification limits (LOQs) of 2.57, 1.28, 1.28, 1.88, 4.16, 4.16 and 4.18 ng mL^{-1} for *d*TK, *l*CK, *d*CK, *d*PA, *d*PB, *l*PB and *d*PE, respectively, while *l*PA was not detected in rat plasma due to the carboxylesterase(s)-mediated hydrolysis. In addition, the validated system was satisfactorily applied to characterize the pharmacokinetic properties of those components in normal and chronic obstructive pulmonary disease (COPD) rats following oral administration of Qian-hu extract. *d*CK and *l*CK were observed as the main herb-related compounds in plasma. Enantioselectively pharmacokinetic profiles occurred for *d*CK *vs* *l*CK, *d*PA *vs* *l*PA, and *d*PB *vs* *l*PB in either normal or COPD rats. The proposed whole system is expected to be a preferable analytical tool for *in vivo* study of chiral drugs, in particular for the characterization of enantioselectively pharmacokinetic profiles.

1. Introduction

Nowadays, approximately 60% of synthetic drugs currently in clinical use are chiral compounds and 88% of these chiral drugs are used therapeutically as racemic or scalemic mixture (where one enantiomer predominates). It was not surprising to discover that enantiomers initiated different pharmacological actions since chirality is a common feature of biomolecules which generally leads to chiral recognition during interactions between xenobiotics and macromolecules. On the other hand, stereoselective pharmacokinetics of chiral drugs has been abundantly documented [1,2] and also accounts for many enantiospecifically pharmacologic properties. Therefore, there is a great demand for characterizing the plasma concentration difference between enantiomers. Unfortunately, for many racemic drugs, their enantiomeric plasma pharmacokinetic profiles are not currently known due to the limitation of analytical methods.

Chiral LC–MS/MS has become the preferred method for enantiospecifically quantitative analyses, since it allows rapid, sensitive, and reliable analysis for most matrices. However, when complicated biological samples were subjected for LC–MS/MS analysis, sample preparation must possess efficient analyte recovery, overcome drug-protein binding and avoid matrix related ion-suppression in the ion source [3–5]. Solvent protein precipitation (SPP), liquid–liquid extraction (LLE) and solid phase extraction (SPE) have been reported as the commonly employed plasma

* Corresponding author. Tel.: +853 8397 4691; fax: +853 2884 1358.
E-mail address: ytwang@umac.mo (Y. Wang).

0731-7085/$ – see front matter © 2013 Elsevier B.V. All rights reserved.
http://dx.doi.org/10.1016/j.jpba.2013.08.042

preparation means, which always involve several manual processing steps and require relatively large amounts of solvent that must be removed prior to LC–MS/MS analysis, potentially contributing to contamination, recovery errors, and could lead to a large variability. Consequently, there is a growing demand to introduce automated online sample preparation methods to promote the employment of chiral LC–MS/MS for routine testing [6]. To be time-gaining and solvent efficient, "rapid LC" methods warrant the use of "rapid efficient sample preparation" [7]. On-line analyte capture with column switching procedures could improve assay efficiency by reducing required sample volumes and minimizing manual sample preparation steps [8]. Moreover, the commercially available chiral stationary phases work satisfactory in rigorous conditions, which require extremely clean samples to preserve their integrity. Fortunately, the adoption of online SPE column assures transference of clean eluate into chiral column, preventing the degradation of the chiral stationary phases and maintaining the column performance for a longer time, and yielding simpler analysis in a shorter analysis time. Up to now, online SPE–LC–MS/MS techniques have been reported for the analysis of many drugs or drug-candidates, yet none was validated for the simultaneous measurement of several pairs of enantiomers in biological matrices adopting automated online SPE combined chiral column with a column switching procedure.

Angular-type pyranocoumarins (APs) comprise a khellactone skeleton with varied substituents at C-3′ and C-4′ positions. Many APs were revealed as anti-hypertensive drug candidates typically through blocking calcium channels and opening potassium channels [9,10]. Recent studies also supported the prospects of these components in chemotherapy on account of their anti-proliferative, cytotoxic and apoptosis-inducing activities [11,12] along with p-glycoprotein (p-gp) expression suppressing effects [13]. Moreover, several khellactone derivatives have been synthesized to explore potent anti-HIV agent that is effective for multiple reverse transcriptase inhibitor resistant strain [14]. APs, such as praeruptorin A (PA), praeruptorin B (PB) and praeruptorin E (PE), were regarded as the main chemical constituents and the major active components contributing to the activities of Peucedani Radix (Chinese name: Qian-hu), which exhibits a diverse range of biological activities, including, but not limited to, coronary dilatory effect [15], anti-inflammation [16], antitumor-promotion [17] and significantly beneficial effects on both animal models and patients suffered from pulmonary hypertension [18–22]. In particular, solid evidences for the treatment of chronic obstructive pulmonary disease (COPD) have been reported according to widely clinical practices [21,22]. Interestingly, enantioselectivities were observed for the pharmacological effect, metabolism and absorption of PA enantiomers [23–25]. Carboxylesterase(s)-catalyzed hydrolysis was observed for (−)-praeruptorin A (*l*PA) in liver microsomal proteins of rats and humans in the absence of a NADPH-regenerating system, in rat plasma and in Caco-2 cells, while (+)-praeruptorin A (*d*PA) kept intact in those situations [24,25]. The findings obtained *in vitro* strongly indicated enantioselectively pharmacokinetic properties for this type of coumarins *in vivo*.

To the best our knowledge, the online SPE column has not been coupled with chiral column to simultaneously determinate several pairs of enantiomers *in vivo*, and the material basis of Qian-hu for the therapeutical effect on COPD has not been revealed. Therefore, the present study aims to develop an automated method of online SPE coupled to a chiral column and a hybrid quadrupole-linear ion trap-mass spectrometer (online SPE–chiral LC–MS/MS) for simultaneously enantiospecific determination of (+)-*trans*-khellactone (*d*TK), (+/−)-praeruptorin A (*d*/*l*PA), (+/−)-praeruptorin B (*d*/*l*PB) and (+)-praeruptorin E (*d*PE) and their major metabolites, (+/−)-*cis*-khellactone (*d*/*l*CK), in normal and COPD rat plasma.

2. Experimental

2.1. Chemical and reagents

(+)-*trans*-Khellactone (*d*TK, M.W. 262 Da) was prepared by basic hydrolysis of *d*PA following the method described in Ref. [26] and its structure was unambiguously identified using LC–MS/MS and NMR analysis. (−)-*cis*-Khellactone (*l*CK, M.W. 262 Da), (+)-*cis*-khellactone (*d*CK, M.W. 262 Da), (+)-praeruptorin A (*d*PA, M.W. 386 Da), (−)-praeruptorin A (*l*PA, M.W. 386 Da), (+)-praeruptorin B (*d*PB, M.W. 426 Da) and (−)-praeruptorin B (*l*PB, M.W. 426 Da) and (+)-praeruptorin E (*d*PE, M.W. 428 Da) were isolated from Peucedani Radix in our previous report (Fig. 1) [25,27]. All the optical purities were determined as higher than 98% using chiral LC–MS/MS analysis. 7-Ethoxycoumarin (7-EC, purity > 98%), that was adopted as internal standard (IS) for online SPE–chiral LC–MS/MS analysis, was purchased from Sigma–Aldrich Chimie SARL (St. Louis, MO, USA).

HPLC grade of formic acid and acetonitrile were obtained from Merck (Darmstadt, Germany). Deionized water was obtained using a Milli-Q water purification system from Millipore (Bedford, MA, USA). *n*-Propanediol was of analytical grade and obtained from Kaitong Chemical Co. Ltd. (Tianjin, China).

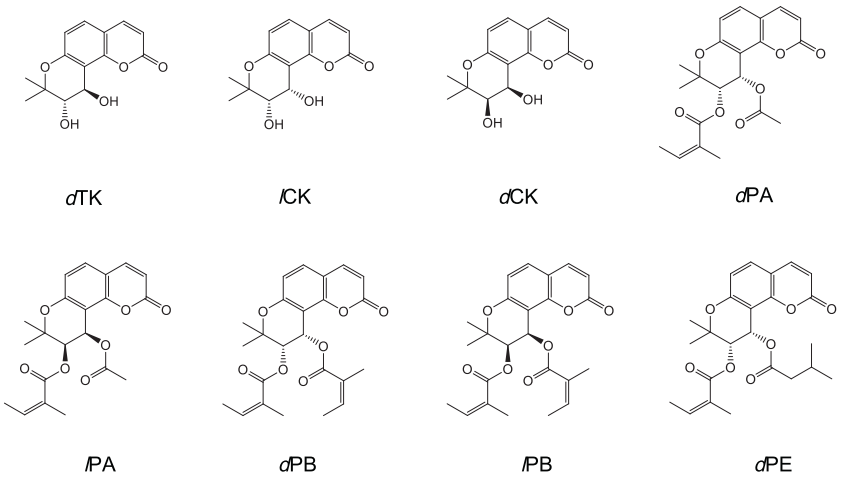

Fig. 1. Chemical structures and international nonproprietary names of the analytes covered by the assay, (+)-*trans*-khellactone (*d*TK), (−)-*cis*-khellactone (*l*CK), (+)-*cis*-khellactone (*d*CK), (+)-praeruptorin A (*d*PA), (−)-praeruptorin A (*l*PA), (+)-praeruptorin B (*d*PB) and (−)-praeruptorin B (*l*PB) and (+)-praeruptorin E (*d*PE).

2.2. Online SPE–chiral LC–MS/MS system setup

The general layout of the online SPE–chiral LC–MS/MS instrumentation setup presented previously was introduced in current study with minor modifications [28]. Briefly, a tandem mass spectrometer (API 4000Q-trap, ABSciex, Forster City, CA, USA), of which Q3 cell can perform as linear ion trap mass spectrometer, was equipped with a Turbo V™ ion source operating in the electro spray ionization (ESI) mode and served as the detector. The HPLC system coupled to that mass spectrometer consisted of a vacuum degasser (G1379B), a binary pump (HPLC pump, G1312B), an autosampler thermostat (G1330B), an autosampler with the injection loop of 40 μL (G1367C) and a column oven (G1316A, all Agilent Technologies, USA), a ten-port valve (VICI Valco Instruments Co. Inc., TX, USA) and a one-channel pump (Varian Pro Star Solvent Module, Varian, PA, USA). ABSciex Analyst Software package Version 1.5.1 was used to control the whole system and for data acquisition and processing.

The one-channel pump (SPE pump) was connected to ten-port valve of the autosampler and responsible for delivering solvent to the SPE column (Strata™-X, 2.0 mm × 20 mm i.d., 5.0 μm particle size; Phenomenex, Torrance, CA, USA) that was maintained at room temperature (25 °C). The binary pump (HPLC pump) was used to deliver mobile phase to the chiral column (Chiralpak AD-RH, 4.6 mm × 150 mm i.d., 5.0 μm particle size, Daicel, Tokyo, Japan) which was thermostated at 45 °C. The outlet of the chiral column was connected to the mass spectrometer ion source. On the other side, the SPE pump delivered 5% aqueous acetonitrile at a flow rate of 1 mL min^{-1} to facilitate the lipophilic constituents of the injected sample being trapped onto the SPE column. After flushing hydrophilic matrix material at loading position for 4 min (Supplemental figure, Fig. S1), the valve was switched to elution position, maintained for another 21 min and the lipophilic matrix components including the analytes were back-flushed using a programmed HPLC condition. The gradient mobile phase consisted of 0.1% HCOOH–H_2O (A) and 0.1% HCOOH–ACN (B) and was delivered at a flow rate of 0.65 mL min^{-1} as: 0–4 min, 15–15% B; 4–14 min, 15–60% B; 14–15 min, 60–70% B; 15–20 min, 70–75% B; 20–23 min, 75–90% B; 23–23.1 min, 90–15% B; 23.1–25 min, 15% B. Enantiomeric elution order was determined by injecting each optical pure enantiomer into the online SPE–chiral LC–MS/MS system separately. The switching valve settings were illustrated in Supplemental figure (Fig. S1).

Supplementary data associated with this article can be found, in the online version, at http://dx.doi.org/10.1016/j.jpba.2013.08.042.

The mass spectrometer was operated in the multiple reaction monitoring (MRM) mode. ESI ion optics was tuned using standard polypropylene glycol (PPG) dilution solvent. Nitrogen was used as the nebulizer, heater, curtain and collision gas. The ion source operating in the positive ion mode with an ion-spray voltage of 5500 V was heated to 500 °C. Gas setting: nebulizer gas (GS1) as 50 psi, heater (GS2) as 50 psi and curtain gas (CUR) as 20 psi. Two precursor-product ion transitions were recorded for each analyte and one for internal standard. Since the isotope-labeled internal standard is not commercially available, 7-EC that is an analog of these angular-type pyranocoumarins was chosen as internal standard. For the MRM parameters and analyte retention time, see Table 1, while the dwell time, entrance potential (EP) and collision cell exit potential (CXP) of each ion transition was fixed at 120 ms, 10 V and 12 V, respectively. In addition, the MRM mode was also adopted as the survey experiment to trigger two separated enhanced product ion (EPI) scans according to an information dependent acquisition (IDA) procedure with the threshold of 500 cps. The parameters for EPI scan were set as follows: declustering potential (DP) as 130 V, collision energy (CE) as 30 eV and collision energy spread (CES) as 20 eV.

The Analyst software quantification module was used to generate the quantification method including peak detection, peak integration, and analyte quantification. Within the automated Analyst Classic integration algorithm the smoothing factor was set to 2 and the bunching factor to 1 for all investigated peaks. Calibration function generation was carried out by plotting the peak area ratio of an analyte and its respective internal standard against the corresponding analyte–internal standard concentration ratio. A $1/x$ weighting function was used for the linear regression of each analyte.

2.3. Method validation

The method validation was carried out in accordance with internationally accepted criteria [29]. The linearity was evaluated using external calibration curves with more than seven calibration levels for each analyte prepared in triplicate.

2.3.1. Preparation of calibration standards and quality control samples

Standard stock solutions of *d*TK (2.62 mg mL^{-1}), *l*CK (2.62 mg mL^{-1}), *d*CK (2.62 mg mL^{-1}), *d*PA (1.93 mg mL^{-1}), *l*PA (1.93 mg mL^{-1}), *d*PB (4.26 mg mL^{-1}), *l*PB (4.26 mg mL^{-1}) and *d*PE (4.28 mg mL^{-1}) were prepared by dissolving each accurately weighed reference compound in an appropriate volume of DMSO, and used to make up the standard mixed stock solution (final content: 0.262 mg mL^{-1} for *d*TK, *d*CK and *l*CK, 0.386 mg mL^{-1} for *d*PA and *l*PA, 0.426 mg mL^{-1} for *d*PB and *l*PB, and 0.428 mg mL^{-1} for *d*PE). A series of working standard solutions and quality control (QC) spiking solutions were prepared by serial dilution of the standard mixed stock solution using DMSO. All the standard solutions were kept at 4 °C until use.

Aliquots of the working mixed standard solutions were spiked with pooled blank rat plasma to yield respective calibration range for each investigated component (Table 2) and stored at −20 °C in 2 mL polypropylene round bottom sample tube (Eppendorf, Hamburg, Germany) until use. The quality control (QC) samples at low, medium and high concentration levels (Table 3) for each analyte were prepared in the same manner and held under identical conditions.

Each of the prepared calibrators and QC samples was aliquoted with 4 volumes of phosphate buffer (pH 7.4) that contained 190 ng mL^{-1} internal standard.

2.3.2. Selectivity and specificity

This assay of selectivity was carried out to identify potential chromatographic interference from endogenous entities at the peak regions of the analytes and internal standard. Chromatographic peaks from plasma samples were compared with the authentic standards by the retention times and MS^2 spectra obtained by the EPI scans.

2.3.3. Linearity and LOQ

Each calibration level was tested in triplicate. To obtain an acceptable deviation for all of the concentration levels, the standard curves were fitted by a weighed ($1/x$) least squares linear regression method through by plotting the peak area ratio of each analyte to IS *versus* the theoretical plasma concentrations over the calibration concentration range. The acceptance criterion for each calibration curve was a correlation coefficient (r) of 0.99 or better and a back-calculated standard concentration within a 15% deviation from the nominal value except at the limit of quantification. The LOQ, defined as the lowest concentration in the standard curve, was determined by an intermediate repeatability experiment. LOQ confirmation (inter-day imprecision less than 20%, inter-day

Table 1
Retention times of investigated analytes, precursor-to-product ion transitions and parameters of multiple-reaction monitoring (MRM) mode.

Analyte	Selected reaction ion type	Retention time (min)	Precursor/product ion (*m*/*z*)	DP (V)	CE (eV)
*d*TK	Quant	12.9	263.1/203.1	86	21
	Qual		263.1/245.1	86	16
*l*CK	Quant	14.1	263.1/203.1	86	21
	Qual		263.1/245.1	86	16
*d*CK	Quant	14.9	263.1/203.1	86	21
	Qual		263.1/245.1	86	16
*d*PA	Quant	18.6	409.0/227.1	130	37
	Qual		409.0/245.1	130	24
*l*PA	Quant	19.5[a]	409.0/227.1	130	37
	Qual		409.0/245.1	130	24
*d*PB	Quant	19.9	449.1/227.1	130	34
	Qual		449.1/245.1	130	31
*l*PB	Quant	20.3	449.1/227.1	130	34
	Qual		449.1/245.1	130	31
*d*PE	Quant	20.1	451.1/227.1	130	35
	Qual		451.1/245.1	130	32
7-EC[b]	Quant	18.3	191.1//163.5	60	25

*d*TK: (+)-*trans*-khellactone; *l*CK: (−)-*cis*-khellactone; *d*CK: (+)-*cis*-khellactone; *d*PA: (+)-praeruptorin A; *l*PA: (−)-praeruptorin A; *d*PB: (+)-praeruptorin B; *l*PB: (−)-praeruptorin B; *d*PE: (+)-praeruptorin E.
DP, declustering potential; CE, collision energy; Quant, quantifier; Qual, qualifier.
[a] *l*PA was not observed in plasma.
[b] 7-EC acted as the internal standard.

Table 2
Linear regression data, limits of quantification (LOQ) for all investigated analytes.

Analyte	Linear regression data			LOQ (ng mL^{-1})
	Regression equation	*r*	Test range (ng mL^{-1})	
*d*TK	$y = 0.00097x + 0.0351$	0.9990	2.57–1315	2.57
*l*CK	$y = 0.000357x + 0.00094$	0.9953	1.28–1315	1.28
*d*CK	$y = 0.000309x + 0.000586$	0.9976	1.28–1315	1.28
*d*PA	$y = 0.00378x + 0.00779$	0.9985	1.88–1930	1.88
*d*PB	$y = 0.00167x + 0.0087$	0.9998	4.16–2130	4.16
*l*PB	$y = 0.00144x + 0.00549$	0.9957	4.16–2130	4.16
*d*PE	$y = 0.00288x + 0.0228$	0.9959	4.18–2140	4.18

*d*TK: (+)-*trans*-khellactone; *l*CK: (−)-*cis*-khellactone; *d*CK: (+)-*cis*-khellactone; *d*PA: (+)-praeruptorin A; *l*PA: (−)-praeruptorin A; *d*PB: (+)-praeruptorin B; *l*PB: (−)-praeruptorin B; *d*PE: (+)-praeruptorin E.

Table 3
Inter-day and intra-day ($n = 6$) performance parameters of low, medium and high level quality control samples for all analytes.

Analyte	Concentration level	Concentration (ng mL^{-1})	Intra-day (%)	Inter-day (%)
*d*TK	High	1310	1.1	2.7
	Medium	163.8	3.3	5.6
	Low	40.4	1.9	3.8
*l*CK	High	1310	6.8	9.3
	Medium	163.8	2.2	5.3
	Low	40.4	1.9	3.6
*d*CK	High	1310	5.7	8.4
	Medium	163.8	2.3	3.9
	Low	40.4	2.3	4.3
*d*PA	High	1930	1.8	4.0
	Medium	241.3	2.0	5.1
	Low	60.3	2.0	6.3
*d*PB	High	2130	4.9	7.9
	Medium	266.3	3.2	3.9
	Low	66.6	2.3	3.7
*l*PB	High	2130	4.4	7.2
	Medium	266.3	3.5	3.7
	Low	66.6	1.5	4.9
*d*PE	High	2140	3.3	7.6
	Medium	267.5	3.8	8.1
	Low	66.9	1.7	5.7

*d*TK: (+)-*trans*-khellactone; *l*CK: (−)-*cis*-khellactone; *d*CK: (+)-*cis*-khellactone; *d*PA: (+)-praeruptorin A; *l*PA: (−)-praeruptorin A; *d*PB: (+)-praeruptorin B; *l*PB: (−)-praeruptorin B; *d*PE: (+)-praeruptorin E.

Table 4
Pharmacokinetic parameters of investigated analytes in rats of normal and chronic obstructive pulmonary disease (COPD) groups.

Analyte	Group	C_{max} (ng mL^{-1})	$T_{1/2}$ (h)	AUC_{0-t} (ng h mL^{-1})
*d*TK	Normal	55.5 ± 31.3	8.77 ± 1.15	488 ± 108
	COPD	51.8 ± 22.4	12.8 ± 9.30	543 ± 179
*l*CK	Normal	468 ± 233	7.00 ± 1.42	3557 ± 902
	COPD	362 ± 224	4.79 ± 0.75*	2910 ± 1134
*d*CK	Normal	112 ± 26.9#	7.01 ± 1.40	850 ± 169#
	COPD	295 ± 201*	7.09 ± 1.59#	1414 ± 537#
*d*PA	Normal	19.8 ± 11.3	27.8 ± 34.2	57.8 ± 27.0
	COPD	18.0 ± 6.6	9.65 ± 5.96	149 ± 60.5*
*d*PB	Normal	10.3 ± 5.42	8.77 ± 1.15	132 ± 34.8
	COPD	12.1 ± 5.15	12.8 ± 9.30	213 ± 35.0*
*d*PE	Normal	5.35 ± 0.41	8.77 ± 1.15	129 ± 15.9
	COPD	10.4 ± 3.23*	12.8 ± 9.30	224 ± 29.9*

*d*TK: (+)-*trans*-khellactone; *l*CK: (−)-*cis*-khellactone; *d*CK: (+)-*cis*-khellactone; *d*PA: (+)-praeruptorin A; *l*PA: (−)-praeruptorin A; *d*PB: (+)-praeruptorin B; *l*PB: (−)-praeruptorin B; *d*PE: (+)-praeruptorin E.
Significant difference between enantiomers was observed ($P < 0.05$, *t*-test).
* Significant difference between normal and COPD rats was observed ($P < 0.05$, *t*-test).

inaccuracy less than ±20%) was achieved with full calibration sample sets.

2.3.4. Accuracy and precision

Accuracy and intra- and inter-day precision were assessed by analyzing three consecutive batches containing calibration curve standards and six replicates of each QC level (low, medium and high), respectively. The accuracy was expressed as (observed concentration/nominal concentration) × 100% (RE) and acceptable at the case of RE within ±15%, while the relative standard deviation (RSD, %) were expected to be within ±15% to be acceptable for precision.

2.3.5. Stability

The stability of each stock solution was determined by preparing fresh stock solution from the reference material and comparing the absolute response of the 100-fold diluted (using phosphate buffer, pH 7.4) fresh solution with that of the 100-fold diluted (using phosphate buffer, pH 7.4) two-month stored solution.

Three aliquots of low, medium and high QC samples were analyzed for short-term stabilities, three cycles of freeze–thaws and long-term stabilities assays of the analytes. Short-term stability was assessed by maintaining the QC samples at room temperature for 4 h before analysis. Freeze–thaw cycle stability assay was carried out *via* repeatedly freezing (store at −20 °C for 24 h) and thawing (completely thaw at room temperature) QC samples for three cycles before analysis. Long-term stability was evaluated by storing QC samples at −20 °C for two weeks before thawing and extraction.

2.3.6. Matrix effect and extraction efficiency assessment

Matrix effects were investigated using qualitative oriented online SPE–LC–MS/MS post LC infusion experiments [30]. Briefly, diluted blank rat plasma was subjected for online SPE–LC–MS/MS analysis and the eluent from chiral column was introduced into the T-piece mounted on ion source housing of the MS instrument. Meanwhile, high, medium or low concentration QC sample, which was prepared by diluting the standard mixed solution with 50% aqueous acetonitrile containing 190 ng mL^{-1} internal standard, was also delivered into the T-piece at the rate of 10 μL min^{-1} using a syringe pump (Harvard HA22I, Instech Laboratories, Inc. Plymouth Meeting, PA, USA). The ion yield attenuation of each analyte was used for qualitative assessment of matrix effect.

Online SPE extraction efficiency was qualitatively and quantitatively assessed using the method described in Ref. [31]. In this assay, the three QC concentration levels were obtained by diluting the standard mixed solution using 100% water that contained 190 ng mL^{-1} internal standard. The outlet of the SPE column was directly connected with the T-piece instead of being deserted to check whether the analytes could be eluted during the loading duration (0–4 min). For the sake of quantitative assessment, independent experiments using deionized water with the three QC samples were performed on three different days with threefold analysis repetitions at each day. The analyte signals afforded by the online SPE–LC–MS/MS analyses proposed above were defined as Set B. On the other hand, the analyte signals (peak areas) obtained by direct injection of analytes into the chiral column were defined as Set A. Thus, the process efficiency (%) was calculated as B/A × 100.

2.4. In vivo sample preparation

The whole *in vivo* protocol was approved by the Animal Ethics Committees of Sun Yat-sen University (Guangzhou, China) and University of Macau (Macao, China). SPF-grade Wistar male rats (Certificate No. SCXK2011-0029) were provided by Sun Yat-sen University Laboratory Animal Center and acclimated in laboratory for one week prior to the experiments. Animals were housed at the temperature of 23 ± 1 °C with a 12-h light/dark cycle and relative humidity of 50%. Standard diet and water were provided *ad libitum*. Rats were divided randomly into normal and chronic obstructive pulmonary disease (COPD) groups ($n = 6$). Each rat from COPD group was exposed to cigarette smoke 2 h/day for 4 weeks combined intratracheal treatment with lipopolysaccharides (LPS) from *E. coli* (200 μg kg^{-1}, 20 μg mL^{-1} dissolved in saline) [32].

A well established *in vivo* pharmacokinetic protocol in rat [33] was applied in the present study. The day before administration, a jugular vein cannula (polyethylene, o.d. 0.8 mm, i.d. 0.4 mm) was implanted for receiving p.o. dosing blood sampling under light anesthesia with diethyl ether. After cannulation, all the rats were allowed to recover and fasted overnight with free access to water. A single dose of Qian-hu extract (500 mg kg^{-1}) in normal saline containing 50% *n*-propanediol was orally treated to each rat. Then 0.25 mL of blood samples were collected into pre-heparinized Eppendorf tubes at appropriate time points of 0.08, 0.16, 0.33, 0.5, 0.75, 1, 1.5, 2, 3, 5, 8, 12, 24 and 36 h. After each collection, 0.25 mL of saline containing 40 IU of heparin·mL^{-1} was adopted to flush the cannula immediately to compensate for blood loss and prevent clotting after each blood sampling. Each blood sample was immediately centrifuged at approximately 3000 × *g*, 4 °C for 10 min and Qian-hu-treated plasma samples were

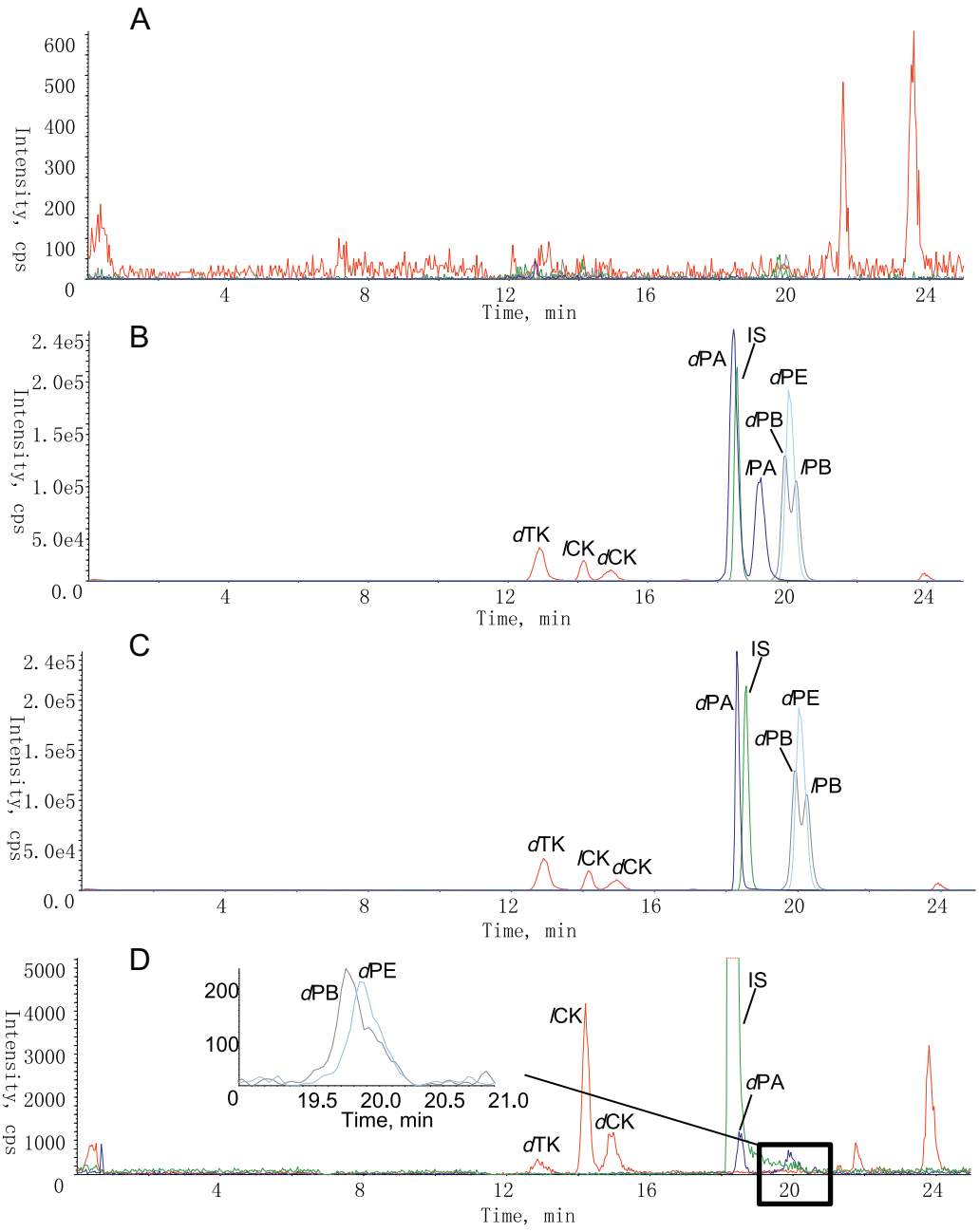

Fig. 2. Representative chromatograms of pooled blank plasma (A), *d*TK, *l*CK, *d*CK, *d*PA, *d*PB and *d*PE spiked with phosphate buffer (B) or pooled blank rat plasma (C), and the plasma sample from a rat at 1 h after oral treatment (D).

harvested. Each 50 μL aliquot of supernatant plasma layer was transferred into another tube and stored at −20 °C refrigerator until it was mixed thoroughly with 200 phosphate buffer (pH 7.4) containing 190 ng mL^{-1} of internal standard and subjected to analyses on the online SPE–chiral LC–MS/MS system at an injection volume of 40 μL.

2.5. Analysis of pharmacokinetic parameters

Individual animal plasma concentrations *versus* time data were subjected to a non-compartmental analysis (WinNonlin 5.1, Pharsight, Moutain View, CA, USA). The observed and calculated pharmacokinetic parameters include the maximum plasma concentration (C_{max}), the terminal elimination half-life ($t_{1/2}$), area under the plasma concentration-time curve from time 0 to time t ($AUC_{0\rightarrow t}$).

2.6. Statistical analysis

The pharmacokinetic parameters of *d*TK, *l*CK, *d*CK, *d*PA, *d*PB and *d*PE following administration of Qian-hu extract in normal and COPD rats were compared using Student's *t*-test. *P*-values less than 0.05 were considered significant. All results are expressed as mean ± SD.

3. Results and discussion

3.1. Optimization of LC–MS/MS parameters

The optimized chromatography and mass spectrometry parameters are summarized in Section 2 and in Table 1. The final method had an analysis time of 25 min (injection to injection interval)

with analytes and internal standards eluting at a retention time window of 12–23 min. For the time-saving purpose, the chiral column was equilibrated using 15% aqueous acetonitrile when the whole system was maintained at loading phase. SPE loading conditions were followed the method published previously [34]. Based on Q1 and product ion scans of the analytes (syringe pump-based infusion experiments) MRM ion transitions for analytes and internal standards were selected using the "quantitative optimization" algorithm provided by the Analyst software. Any precursor to product ion transition based on non-selective ion reactions (*i.e.*, loss of water) was excluded whenever possible. All selected precursor/product ion transitions were checked for their selectivity by using analyte free-blank rat plasma samples and for sensitivity using analyte free-blank rat plasma samples spiked with those investigated reference compounds. Finally, two precursor/product ion pairs per analyte (quantifier and qualifier ions) and one for internal standard were chosen, with the latter one being matched to the quantifier ion transition in respect to collision energy and declustering potential voltages. For detailed information, see Table 1. Ion source parameters such as temperature and gas flows were optimized by infusing the analyte and the IS into the mobile phase by using a T-piece mounted between the HPLC column outlet and the ion source of the mass spectrometer. Positive ESI mode was found superior over APCI or negative ESI mode. Precursor ion yield was found to be significantly better at higher ion-spray voltages, finally 5500 V were selected. Ion source gas flows and ion source temperature were followed the typical range for the LC effluent chosen.

3.2. Method validation

3.2.1. Selectivity and specificity

Retention times of the eight analytes and IS were summarized in Table 1. Fig. 2 illustrated typical chromatograms from blank plasma, phosphate buffer spiked with mixed standards, plasma spiked with mixed standard, and plasma obtained 1 h after administration. Each analyte was found to be free from interferences in the retention time window of the analytes (Fig. 2). Satisfactory enantiomeric separation was achieved for most enantiomers on the current online SPE–chiral LC–MS/MS system. All the findings indicated that the developed method exhibited high selectivity and specificity. Interestingly, *l*PA was observed in phosphate buffer, yet absent in plasma. As we reported previously [25], hydrolysis of *l*PA could be crucially mediated by the carboxylesterase(s) in rat plasma to yield the two hydrolyzed products of 3′-angeloxyl-*cis*-khellactone and *cis*-4′-angeloxylkhellactone. In addition, this compound could only be detected in the first 5 min when *l*PA was *i.v.* administration [35]. Therefore, the levorotatory enantiomer of praeruptorin A could not be observed after oral administration of Qian-hu extract with no surprise. However, the hydrolysis of *l*PA cannot be catalyzed by the carboxylesterase(s) in human plasma (data not shown), suggesting significant species difference between rats and human beings. In the developed method, baseline separation was achieved for the levoisomer and dextroisomer of PA, indicating that this method could also be applied for the pharmacokinetic characterization of Qian-hu in human plasma.

3.2.2. Linearity, accuracy and precision

Correlation coefficients (r) of calibration curves in all inter-run cases were greater than 0.99 over the concentration ranges of 2.57–1315 ng mL^{-1} for *d*TK, 4.16–2130 ng mL^{-1} for *d*PB, 4.16–2130 ng mL^{-1} for *l*PB and 4.18–2140 ng mL^{-1} for *d*PE, and 1.28–1315 ng mL^{-1} for *l*CK, 1.28–1315 ng mL^{-1} for *d*CK and 1.88–1930 ng mL^{-1} for *d*PA, respectively (Table 2). A weight of $1/x$ was applied to minimize the relative error for the curve fitting. The LOQ of *d*TK, *l*CK, *d*CK, *d*PA, *d*PB, *l*PB and *d*PE were determined as 2.57, 1.28, 1.28, 1.88, 4.16, 4.16 and 4.18 ng mL^{-1} in this assay, respectively (Table 2).

The results meet the pertinent guidelines [29]. For all the eight target compounds, accuracy located at the range of 90.3–109.6%, and the RSDs of intra- and inter-day precisions were lower than 5% for all analytes. Table 3 presented the results for precision evaluation. Those findings indicated that the developed method is a precise and accurate method.

3.2.3. Matrix effects and extraction efficiency

Online SPE–LC–MS/MS and post LC column infusion experiments were inspected for the occurrence of interfering peaks or ion-suppression troughs. Each of the investigated components was found to be free from interferences in the retention time window of the analytes indicating the matrix effects of the developed method could be ignored for the quantitative analyses of analytes.

Deionized water was fortified with the analytes at high, medium and low concentration levels, respectively, and the mixtures were employed to address the extraction efficiency assay. The numbers for the process efficiency were positive with a mean of 109.3 ± 4.7% (mean ± standard deviation), indicated that the loading procedure did not induce the loss of the analytes.

3.2.4. Stability

The results of stability assays for stock solution suggested that all *d*TK, *l*CK, *d*CK, *d*PA, *d*PB, *l*PB and *d*PE could stay table in DMSO within two months when they were kept at 4 °C.

The deviations of the measured concentrations from the standard ones in the stability tests were within the ±10% assay variability limit. This result indicated that *d*TK, *l*CK, *d*CK, *d*PA, *d*PB, *l*PB and *d*PE components were stable on the bench at room temperature (25 °C) for 4 h, during residence time in the auto-sampler, at the end of three consecutive freeze–thaw cycles and after long-term storage, while *l*PA was not detected in plasma due to the crucial carboxylesterase(s)-mediated hydrolysis. The internal standard working solutions stable over 7 days at −20 °C. Hence, internal standard working solutions and sample preparation solutions have to be prepared weekly.

In addition, the impacts from carryover and re-injection were also assessed and the results suggested that influences of these two items could be ignored due to the quite low levels of them.

3.3. Pharmacokinetic application

The developed online SPE–chiral LC–MS/MS method for simultaneous quantification of eight APs was employed in a pharmacokinetic evaluation. *d*CK and *l*CK were observed as the main herb-related compounds in both normal and COPD rats. *l*PA was not observed in *in vivo* samples, while its antipode (*d*PA) was detectable in most of the pharmacological samples, suggesting obvious enantioselectivity between these enantiomers. On the other side, *l*PB, which was much less abundant than its antipode in extract, was only detected in quite low concentrations in some certain time points, but *d*PB was observed at higher concentrations. As a consequence, enantiospecific pharmacokinetic profiles occurred for both praeruptorin A and praeruptorin B. In view of the distinct pharmacological properties between *d*PA and *l*PA, *d*PA was regarded as the eutomer of PA in combination of the enantioselective metabolism and pharmacokinetics of the two enantiomers of PA, while *l*PA was characterized as the distomer.

The concentration–time curves for *d*TK, *l*CK, *d*CK, *d*PA, *d*PB and *d*PE are shown in Fig. 3 after an oral dose of 500 mg kg^{-1} Qian-hu extract in the normal and COPD rats. The mean concentration–time data were analyzed using noncompartmental analysis with the assistance of Winnonlin 5.0.1 software. The pharmacokinetic parameters are presented in Table 4 and compared between

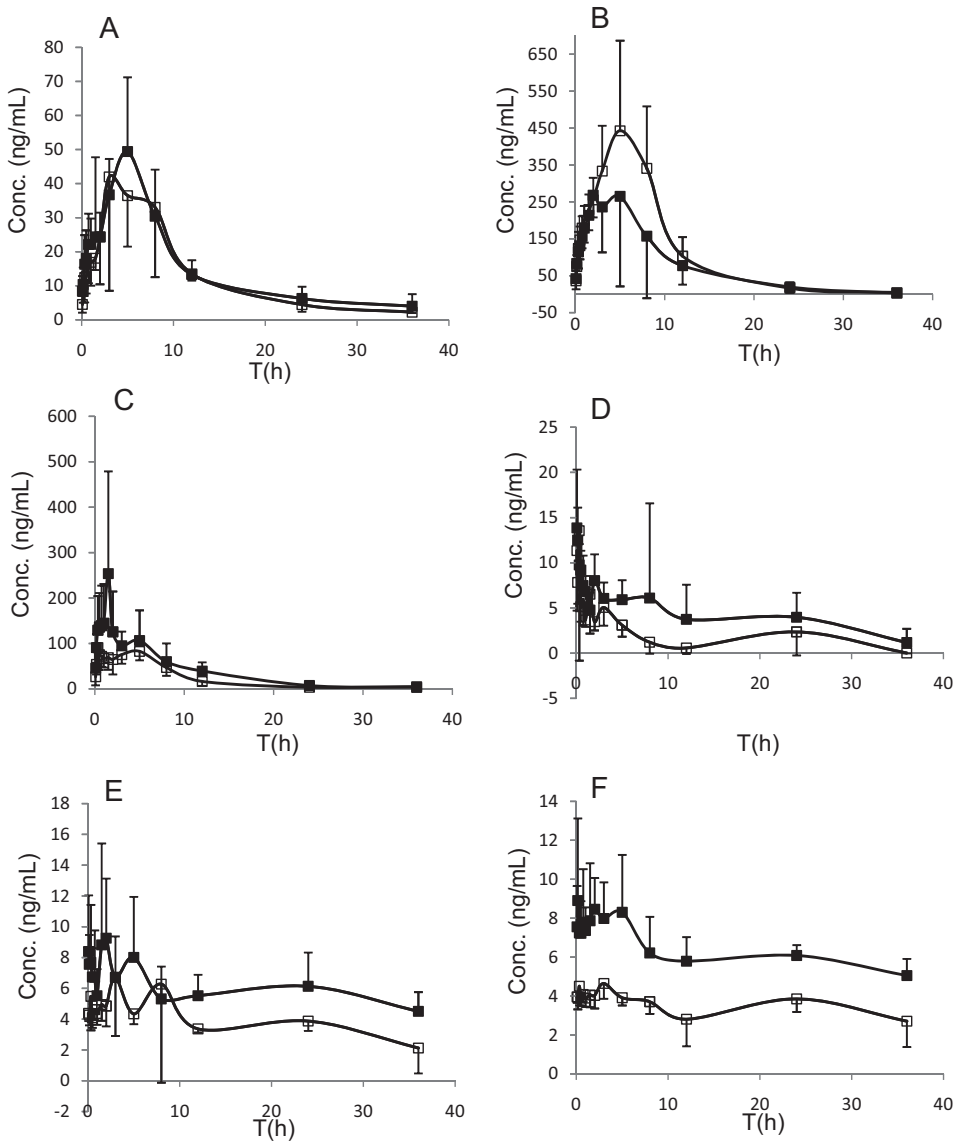

Fig. 3. Mean (±SD, $n = 6$) concentration–time profiles of *d*TK (A), *l*CK (B), *d*CK (C), *d*PA (D), *d*PB (E) and *d*PE (F) in normal (hollow) and chronic obstructive pulmonary disease (COPD) (solid) rat plasma following oral administration of Qian-hu extract.

the two groups using *t*-test to screen the potent significant difference. *l*CK, which is the end hydrolyzed product of (3′S, 4′S)-*cis*-khellactone derivates (such as *d*PA, *d*PB, *d*PE), was determined as the major herb-related component *in vivo* and exhibited the highest C_{max} and AUC_{0-t}. The dextroisomer of *cis*-khellactone (*d*CK), which is the end metabolic product of (3′R, 4′R)-*cis*-khellactone derivates (such as *l*PA, *l*PB, *l*PE), was detected as the secondly abundant components in plasma. The *t*-test results indicate that significant differences occur for C_{max} in normal rats (*l*CK: 468 ± 233 *vs* *d*CK: 362 ± 224, ng mL^{-1}), $t_{1/2}$ in COPD rats (*l*CK: 4.79 ± 0.751 *vs* *d*CK: 7.09 ± 1.59, h), and AUC_{0-t} in both normal and COPD groups between the levoisomer and dextroisomer of *cis*-khellactone. When the crude extract was mixed with phosphate buffer and injected into the developed system, enantioselective preference occurred for the dextrorotatory forms of PA, PB and PE (data not shown). The generation rates of *l*CK and *d*CK from *d*PA and *l*PA, respectively, were characterized in microsomal protein, and the findings indicating that both *d*PA and *l*PA exhibited quick elimination while *l*CK and *d*CK showed rapid generation [25].

In addition, significant differences were observed for $t_{1/2}$ of *l*CK (normal: 7.00 ± 1.42 *vs* COPD: 4.79 ± 0.751, h), C_{max} of *d*CK (normal: 112 ± 26.9 *vs* COPD: 295 ± 201, ng mL^{-1}) and *d*PE (normal: 5.35 ± 0.41 *vs* COPD: 10.37 ± 3.23, ng mL^{-1}), and AUC_{0-t} of *d*PA (normal: 57.8 ± 27.0 *vs* COPD: 149 ± 60.5, ng h mL^{-1}), *d*PB (normal: 132 ± 34.8 *vs* COPD: 213 ± 30.5, ng h mL^{-1}) and *d*PE (normal: 129 ± 15.9 *vs* COPD: 224 ± 29.9, ng h mL^{-1}) between normal rats and COPD rats, indicating that the treatment with LPS and cigarette smoke could affect the absorption, metabolism and/or some other step of xenobiotics. Further studies are ongoing in our laboratory on comparing the activities and expression of transporters, p-gp for instance, and drug metabolizing enzymes, such as cytochrome P450 (CYP450) between the COPD rats and normal rats, which are expected to provide meaningful evidences and clues for the discriminations observed in current study.

4. Conclusion

A novel, simple, reliable and rapid online SPE–chiral LC–MS/MS assay for simultaneous quantification of eight angular-type pyranocoumarins, including three pairs of enantiomers in rat plasma, was successfully developed, fully validated and satisfactorily applied to characterize the pharmacokinetic properties of *d*TK,

*l*CK, *d*CK, *d*PA, *d*PB, *l*PB and *d*PE in normal and chronic obstructive pulmonary disease (COPD) rats following oral administration of Qian-hu extract. Since the metabolites of enantiomers are always enantiomerically enriched components, it is necessary to simultaneously monitor several pairs of enantiomers *in vivo* using enantiospecific means. As a consequence, the proposed method is expected to be a preferable analytical choice for quantitative analysis of chiral drugs and their metabolites in biological matrices without any further sample processing during the characterization of enantioselectively pharmacokinetic and metabolic profiles.

Acknowledgement

The authors acknowledge financial support from the National Basic Research Program of China 973 program (Grant no. 2009CB522707).

References

[1] H. Shiohira, N. Yasui-Furukori, S. Yamada, T. Tateishi, Y. Akamine, T. Uno, Hydroxylation of R(+)- and S(−)-omeprazole after racemic dosing are different among the CYP2C19 genotypes, Pharm. Res. 29 (2012) 2310–2316.
[2] N.J. Antunes, R.C. Cavalli, M.P. Marques, V.L. Lanchote, Stereoselective determination of metoprolol and its metabolite α-hydroxymetoprolol in plasma by LC–MS/MS: application to pharmacokinetics during pregnancy. Chirality 25 (2013) 1–7.
[3] R. Bakhtiar, T.K. Majumdar, Tracking problems and possible solutions in the quantitative determination of small molecule drugs and metabolites in biological fluids using liquid chromatography–mass spectrometry, J. Pharmacol. Toxicol. Methods 55 (2007) 262–278.
[4] J.M. Kremer, J. Wilting, L.H. Janssen, Drug binding to human alpha-1-acid glycoprotein in health and disease, Pharmacol. Rev. 40 (1988) 1–47.
[5] U. Kragh-Hansen, Molecular aspects of ligand binding to serum albumin, Pharmacol. Rev. 33 (1981) 17–53.
[6] M. Vogeser, C. Seger, A decade of HPLC–MS/MS in the routine clinical laboratory – goals for further developments, Clin. Biochem. 41 (2008) 649–662.
[7] R.A. Trenholm, B.J. Vanderford, S.A. Snyder, On-line solid phase extraction LC–MS/MS analysis of pharmaceutical indicators in water: a green alternative to conventional methods, Talanta 79 (2009) 1425–1432.
[8] T.M. Dodgen, A.D. Cromarty, M.S. Pepper, Quantitative plasma analysis using automated online solid-phase extraction with column switching LC–MS/MS for characterising cytochrome P450 2D6 and 2C19 metabolism, J. Sep. Sci. 34 (2011) 1102–1110.
[9] N.C. Zhao, W.B. Jin, X.H. Zhang, F.L. Guan, Y.B. Sun, H. Adachi, T. Okuyama, Relaxant effects of pyranocoumarin compounds isolated from a Chinese medical plant Bai-Hua Qian-Hu, on isolated rabbit tracheas and pulmonary arteries, Biol. Pharm. Bull. 22 (1999) 984–987.
[10] S.L. Zhang, J.M. Li, Q.H. Xiao, A.H. Wu, Q. Zhao, G.R. Yang, K.Y. Zhang, Effect of dl-praeruptorin A on ATP sensitive potassium channels in human cortical neurons, Acta Pharmacol. Sin. 22 (2001) 813–816.
[11] T. Liang, W. Yue, Q. Li, Chemopreventive effects of *Peucedanum praeruptorum* Dunn and its major constituents on SGC7901 gastric cancer cells, Molecules 15 (2010) 8060–8071.
[12] W.F. Fong, J.X. Zhang, J.Y. Wu, K.W. Tse, C. Wang, H.Y. Cheung, M.S. Yang, Pyranocoumarin(±)-4′-O-acetyl-3′-O-angeloyl-*cis*-khellactone induces mitochondrial-dependent apoptosis in HL-60 cells, Planta Med. 70 (2004) 489–895.
[13] J.Y. Wu, W.F. Fong, J.X. Zhang, C.H. Leung, H.L. Kwong, M.S. Yang, D. Li, H.Y. Cheung, Reversal of multidrug resistance in cancer cells by pyranocoumarins isolated from Radix Peucedani, Eur. J. Pharmacol. 473 (2003) 9–17.
[14] L. Huang, X. Yuan, D. Yu, K.H. Lee, C.H. Chen, Mechanism of action and resistant profile of anti-HIV-1 coumarin derivatives, Virology 332 (2005) 623–628.
[15] H.M. Chang, P.P.H. But, S.C. Yao, L.L. Wang, S.C.S. Yeung (Eds.), Pharmacology and Applications of Chinese Materia Medica, Vol. 2, World Scientific Publisher, Singapore, 2001, p. 905.
[16] Y.Y. Xiong, F.H. Wu, J.S. Wang, J. Li, L.Y. Kong, Attenuation of airway hyperreactivity and T helper cell type 2 responses by coumarins from *Peucedanum praeruptorum* Dunn in a murine model of allergic airway inflammation, J. Ethnopharmacol. 141 (2012) 314–321.
[17] T. Okuyama, M. Takata, H. Nishino, A. Nishino, J. Takayasu, A. Iwashima, Studies on the antitumor-promoting activity of naturally occurring substances. II. Inhibition of tumor-promoter-enhanced phospholipid metabolism by umbelliferous materials, Chem. Pharm. Bull. 38 (1990) 1084–1086.
[18] S.C. Xi, Y.M. Ruan, L.Z. Zhang, W.S. Si, H.T. Li, Experimental studies on inhibitory effects of Radix Peucedani on hypoxic pulmonary hypertension in rats, Zhongguo Zhong Xi Yi Jie He Za Zhi 16 (1996) 218–220.
[19] R. Zhou, H.L. Wang, X.H. Zhang, J. Xing, C.M. Li, Effects of *Peucedanum* Dunn on hemorrheology and hemodynamics in pulmonary circulation of pulmonary hypertensive rats, Zhongguo Yi Ke Da Xue Xue Bao 23 (2001) 197–200.
[20] Q.Y. Wang, J. Kang, E.R. Li, R.H. Yu, Effect of extract from Baihua Qianhu on the plasma endothelin-1 in patients with hypoxic pulmonary hypertension, Zhongguo Yi Ke Da Xue Xue Bao 30 (2001) 28–30.
[21] J. Kang, R.H. Yu, Effects of Baihuaqianhu on pulmonary hypertension in patients with COPD, Zhongguo Yi Ke Da Xue Xue Bao 23 (1994) 122–125.
[22] Q.Y. Wang, E.R. Li, G.X. Zhao, J. Kang, X.M. Hou, R.H. Yu, Effects of extract from Baihua Qianhu on pulmonary hypertension in patients with chronic obstructive pulmonary emphysema, Zhongguo Yi Ke Da Xue Xue Bao 27 (1998) 588–591.
[23] Z. Xu, X. Wang, Y. Dai, L. Kong, F. Wang, H. Xu, D. Lu, J. Song, Z. Hou, (+/−)-Praeruptorin A enantiomers exert distinct relaxant effects on isolated rat aorta rings dependent on endothelium and nitric oxide synthesis, Chem. Biol. Interact. 186 (2010) 239–246.
[24] W.H. Jing, Y.L. Song, R. Yan, H.C. Bi, P.T. Li, Y.T. Wang, Transport and metabolism of (+/−)-praeruptorin A in Caco-2 cell monolayers, Xenobiotica 41 (2011) 71–81.
[25] Y.L. Song, W.H. Jing, H.Y. Zhao, R. Yan, P.T. Li, Y.T. Wang, Stereoselective metabolism of (+/−)-praeruptorin A, a calcium channel blocker from Peucedani Radix, in pooled liver microsomes of rats and humans, Xenobiotica 42 (2012) 231–247.
[26] X.L. Wu, L.Y. Kong, Z.D. Min, Studies on structure modification of (+)-praeruptorin A, Yao Xue Xue Bao 37 (2002) 527–534.
[27] Y.L. Song, Q.W. Zhang, Y.P. Li, R. Yan, Y.T. Wang, Enantioseparation and absolute configuration determination of angular-type pyranocoumarins from peucedani radix using enzymatic hydrolysis and chiral HPLC–MS/MS analysis, Molecules 17 (2012) 4236–4251.
[28] C. Seger, K. Tentschert, W. Stöggl, A. Griesmacher, S.L. Ramsay, A rapid HPLC–MS/MS method for the simultaneous quantification of cyclosporine A, tacrolimus, sirolimus and everolimus in human blood samples, Nat. Protoc., 44 (2009) 526–534.
[29] U.S. Food and Drug Administration, Bioanalytical Method Validation, in: Guidance for Industry, U.S. Food and Drug Administration, 2001, pp. 1–25.
[30] C. Moser, D. Zoderer, G. Luef, M. Rauchenzauner, L. Wildt, A. Griesmacher, C. Seger, Anal. Bioanal. Chem. 403 (2012) 961–972.
[31] N.H. Schebb, M. Huby, C. Morisseau, S.H. Hwang, B.D. Hammock, Simultaneous online SPE–LC–MS/MS quantification of six widely used synthetic progestins in human plasma, Anal. Bioanal. Chem. 400 (2011) 1359–1366.
[32] Y.C. Nie, H. Wu, P.B. Li, Y.L. Luo, C.C. Zhang, J.G. Shen, W.W. Su, Characteristic comparison of three rat models induced by cigarette smoke or combined with LPS: to establish a suitable model for study of airway mucus hypersecretion in chronic obstructive pulmonary disease, Pulm. Pharmacol. Ther. 25 (2012) 349–356.
[33] R. Yan, G. Lin, N.L. Ko, Y.K. Tam, Low oral bioavailability and pharmacokinetics of senkyunolide A, a major bioactive component in Rhizoma Chuanxiong, in the rat, Ther. Drug Monit. 29 (2007) 49–56.
[34] C. Moser, A. Gschließer, V. Mattle, L. Wildt, A. Griesmacher, C. Seger, An ultra-sensitive online SPE–LC–MS/MS method for the quantification of levonorgestrel released from intrauterine devices, Anal. Bioanal. Chem. 400 (2011) 2655–2662.
[35] Y.L. Song, R.N. Zhou, R. Yan, Y.T. Wang, Stereoselective pharmacokinetics of (±)-praeruptorin A in rats, Drug Metabol. Rev. 43 (2011) S182–S183.